

# POSSIBLE RELATION BETWEEN PERSISTENT EMISSION AND ROTATION MEASURE OF FAST RADIO BURSTS

YUAN-PEI YANG<sup>1</sup>, QIAO-CHU LI<sup>2,3</sup> AND BING ZHANG<sup>4</sup>

<sup>1</sup> South-Western Institute for Astronomy Research, Yunnan University, Kunming, Yunnan, P.R.China; ypyang@ynu.edu.cn;

<sup>2</sup> School of Astronomy and Space Science, Nanjing University, Nanjing 210093, China;

<sup>3</sup> Key laboratory of Modern Astronomy and Astrophysics (Nanjing University), Ministry of Education, Nanjing 210093, China;

<sup>4</sup> Department of Physics and Astronomy, University of Nevada, Las Vegas, NV 89154, USA; zhang@physics.unlv.edu

*Draft version January 30, 2020*

## ABSTRACT

The physical origin of fast radio bursts (FRBs) is still unknown. Multiwavelength and polarization observations of an FRB source would be helpful to diagnose its progenitor and environment. So far only the first repeating source FRB 121102 appears to be spatially coincident with a persistent radio emission. Its bursts also have very large values of the Faraday rotation measure (RM) i.e.,  $|RM| \sim 10^5 \text{ rad m}^{-2}$ . We show that there is a simple relation between RM and the luminosity of the persistent source of an FRB source if the observed RM mostly arises from the persistent emission region. FRB 121102 follows this relation given that the magnetic field in the persistent emission region is highly ordered and that the number of relativistic electrons powering the persistent emission is comparable to that of non-relativistic electrons that contribute to RM. The non-detections of persistent emission sources from all other localized FRB sources are consistent with their relatively small RMs ( $|RM| \lesssim \text{a few} \times 100 \text{ rad m}^{-2}$ ). According to this picture, the majority of FRBs without a large RM are not supposed to have strong associated persistent sources.

*Subject headings:* radiation mechanisms: non-thermal — radio continuum: general

## 1. INTRODUCTION

Fast radio bursts (FRBs) are extragalactic radio transients with millisecond durations, large dispersion measures (DMs) and extremely high brightness temperatures (e.g., Lorimer et al. 2007; Thornton et al. 2013; Chatterjee et al. 2017; CHIME/FRB Collaboration et al. 2019a,c; Bannister et al. 2019; Ravi et al. 2019; Prochaska et al. 2019; Marcote et al. 2020; Fonseca et al. 2020). The physical origin of FRBs is still unknown. Among all the published FRBs (<http://frbcat.org>), the first repeating FRB source, FRB 121102, has special properties including a persistent radio counterpart and a large, evolving Faraday rotation measure (RM) (Chatterjee et al. 2017; Michilli et al. 2018).

FRB 121102 was first discovered with the Arecibo telescope (Spitler et al. 2014). Its repeating behavior was further confirmed and studied with other radio telescopes all over the world, including Karl G. Jansky Very Large Array (VLA), Green Bank Telescope, the Five-hundred-meter Aperture Spherical Telescope (FAST), etc. (e.g. Chatterjee et al. 2017; Zhang et al. 2018; Li et al. 2019a). Thanks to the precise localizations and multi-wavelength follow-up observations, a persistent radio counterpart with luminosity of  $\nu L_\nu \sim 10^{39} \text{ erg s}^{-1}$  at a few GHz was discovered to be coincident with FRB 121102 spatially, and the host galaxy of FRB 121102 was identified as a dwarf galaxy at redshift  $z = 0.193$  (Chatterjee et al. 2017; Marcote et al. 2017; Tendulkar et al. 2017). The RM of FRB 121102 has a very large absolute value, i.e.,  $|RM| \sim 10^5 \text{ rad m}^{-2}$ , which decreased by ten percent during seven months (Michilli et al. 2018). Such a large RM implies that the corresponding magnetic field is orders of magnitude

stronger than that in the interstellar medium (ISM), and the variation RM might be related to the change of the magnetic field configuration or strength along the line of sight (e.g., Zhang 2018; Metzger et al. 2019). The host galaxy of another repeater, FRB 180916.J0158+65 (abbreviated as FRB 180916 as follows), was reported recently by Marcote et al. (2020), which is a nearby massive spiral galaxy at  $z = 0.0337$ . There is no coincident persistent emission above  $3\sigma$  of  $18 \mu\text{Jy}$  at 1.6 GHz for this source, which places an upper limit on the persistent source luminosity  $\nu L_\nu < 7.6 \times 10^{35} \text{ erg s}^{-1}$ . This is at least three order of magnitude lower than that of FRB 121102.

The persistent emission of FRB 121102 could be explained by the radiation from a nebula surrounding an FRB source, e.g. a supernova remnant (SNR) or a pulsar wind nebula (PWN) (e.g., Yang et al. 2016; Murase et al. 2016; Metzger et al. 2017; Margalit & Metzger 2018). Alternatively, it could be associated with a supermassive black hole (e.g. Michilli et al. 2018; Zhang 2018). Yang et al. (2016) and Li et al. (2020) studied the synchrotron-heating process by an FRB source in a self-absorbed synchrotron nebula and found that the observed persistent emission associated with FRB 121102 could be generated via multi-injection of bursts. Dai et al. (2017) and Yang & Dai (2019) suggested that the persistent emission could be generated via an ultra-relativistic PWN sweeping up its ambient medium. Wang & Lai (2019) studied the multi-wavelength afterglow emission from the nebula powered by a repeating or non-repeating FRB central engine.

In this work, we consider the possibility that the persistent emission and the RM of an FRB source originate from the same region. In this scenario, we derive a simple relation between the persistent emission

luminosity and RM, and we find that FRB 121102 falls into the relation. If this applies to all FRBs, our result implies that for most FRBs, which have  $|\text{RM}| \lesssim \text{a few} \times 100 \text{ rad m}^{-2}$  (e.g., Petroff et al. 2017; Bhandari et al. 2018; Caleb et al. 2018; Osłowski et al. 2019; Bannister et al. 2019), would not have detectable persistent emission with the current radio telescopes. This paper is organized as follows. In Section 2, we set up the theoretical framework for the relation between persistent emission and RM of an FRB source. We test the relation with some FRBs with the measurements of persistent emission and RM in Section 3. The results are summarized and discussed in Section 4.

## 2. THE RM- $L_{\nu, \text{MAX}}$ RELATION

Let us consider an FRB propagating in a plasma with number density of non-relativistic electrons  $n_e$ , magnetic field strength  $B$ , and scale length  $R$ . The RM in this region is given by

$$|\text{RM}| = \frac{e^3 \xi_B B}{2\pi m_e^2 c^4} n_e R, \quad (1)$$

where the parameter  $\xi_B$  is defined as  $\xi_B = \langle B_{\parallel} \rangle / \langle B \rangle$ ,  $B_{\parallel}$  is the line-of-sight magnetic field, and the  $\langle \rangle$  sign denotes the average value. For a random magnetic field, one has  $\langle B_{\parallel} \rangle = 0$  and hence,  $\xi_B = 0$ . Notice that in Eq.(1), we abbreviate  $\langle B \rangle$  to  $B$ .

On the other hand, the persistent emission with a continuous non-thermal spectrum is generally explained by synchrotron radiation from relativistic electrons. We assume that the number density of relativistic electrons in this region is  $\zeta_e n_e$ , where  $\zeta_e$  is the ratio between the relativistic and non-relativistic electron numbers<sup>1</sup>. The radiation power and the characteristic synchrotron frequency from a randomly oriented electron with Lorentz factor  $\gamma \gg 1$  in a magnetic field  $B$  are  $P = (4/3)\sigma_T c \gamma^2 B^2 / 8\pi$  and  $\nu = \gamma^2 e B / 2\pi m_e c$ , respectively. Thus, the spectral radiation power is given by  $P_{\nu} \simeq P / \nu = m_e c^2 \sigma_T B / 3e$ , which is independent of  $\gamma$ . Let the total number of relativistic electrons be  $N_e = 4\pi R^3 \zeta_e n_e / 3$ . The maximum specific luminosity is

$$\begin{aligned} L_{\nu, \text{max}} &= N_e P_{\nu} = \frac{64\pi^3}{27} m_e c^2 \frac{\zeta_e}{\xi_B} R^2 |\text{RM}| \\ &\simeq (5.7 \times 10^{29} \text{ erg s}^{-1} \text{ Hz}^{-1}) \zeta_e \xi_B^{-1} \\ &\times \left( \frac{|\text{RM}|}{10^5 \text{ rad m}^{-2}} \right) \left( \frac{R}{0.01 \text{ pc}} \right)^2, \end{aligned} \quad (2)$$

where Eq.(1) has been used. One can see that there is a simple linear relation between  $|\text{RM}|$  and  $L_{\nu, \text{max}}$ , with dependences on the size of the persistent emission regions and the parameters  $\zeta_e$  and  $\xi_B$ . The observed peak flux

for an FRB source at the distance  $D$  is

$$\begin{aligned} F_{\nu, \text{max}} &= \frac{L_{\nu, \text{max}}}{4\pi D^2} = \frac{16\pi^2}{27} m_e c^2 \frac{\zeta_e}{\xi_B} \frac{R^2}{D^2} |\text{RM}| \\ &\simeq 480 \mu\text{Jy} \zeta_e \xi_B^{-1} \left( \frac{|\text{RM}|}{10^5 \text{ rad m}^{-2}} \right) \\ &\times \left( \frac{R}{0.01 \text{ pc}} \right)^2 \left( \frac{D}{1 \text{ Gpc}} \right)^{-2}. \end{aligned} \quad (3)$$

For FRB 121102, the peak flux of the persistent emission is  $\sim 200 \mu\text{Jy}$  (Chatterjee et al. 2017), the RM is  $\sim 10^5 \text{ rad m}^{-2}$  (Michilli et al. 2018), and the persistent source has a projected size constrained to be  $\lesssim 0.7 \text{ pc}$  (Marcote et al. 2017). The flux of the persistent emission source has a variation with a timescale of  $\Delta t_{\text{per}} \sim 10 \text{ day}$  (see Figure 2 of Chatterjee et al. 2017), which further constrains the emission region to  $R \sim c \Delta t_{\text{per}} \simeq 0.01 \text{ pc}$ . These numbers for FRB 121102 match Eq.(3) very well given that  $\xi_B \sim \zeta_e \sim 1$  is satisfied. This result might imply that the large RM of FRB 121102 is physically associated with its large persistent emission luminosity. The condition  $\xi_B \sim 1$  requires that the magnetic field is coherent in large scale, which is consistent with the large RM observation. The condition  $\zeta_e \sim 1$  requires that the number of relativistic and non-relativistic electrons are of the same order. According to Eq.(3), the variation of the persistent emission in the timescale of  $\Delta t_{\text{per}} \sim 10 \text{ day}$  would result in an RM variation. Michilli et al. (2018) reported that the RM of FRB 121102 decreases by  $\sim 10\%$  within seven months. Such a long-term evolution of the observed RM might be due to the change of the magnetic field configuration so that  $\xi_B$  is a function of  $t$  (e.g., Zhang 2018).

The above discussion assumes that both the magnetic field  $B$  and the electron number density  $n_e$  are uniform in a region with scale length  $R$ . If the magnetic field  $B$  and electron number density  $n_e$  satisfy a power-law distribution with radius from the source, the results should be of the same order of magnitude or somewhat lower compared with the uniform case presented in Eq.(3). A detailed discussion is presented in Appendix.

Finally, for a source with the brightness temperature  $T_B$  and scale length  $R$ , the observed flux is  $F_{\nu} = (2kT_B / \lambda^2) (R^2 / D^2)$ . According to Eq.(3), one has

$$\begin{aligned} |\text{RM}| &= \frac{27}{8\pi^2} \frac{\xi_B k T_B}{\zeta_e \lambda^2 m_e c^2} \simeq (0.6 \times 10^5 \text{ rad m}^{-2}) \\ &\times \zeta_e^{-1} \xi_B \left( \frac{T_B}{10^{12} \text{ K}} \right) \left( \frac{\nu}{10 \text{ GHz}} \right)^2. \end{aligned} \quad (4)$$

In general, for an incoherent stationary source, the maximum brightness temperature is  $T_{B, \text{max}} \sim (10^{12} - 10^{13}) \text{ K}$  due to the constraint of inverse Compton (IC) catastrophe (Kellermann & Pauliny-Toth 1969). According to Eq.(4), the observed large RM from FRB 121102 demands a  $T_b$  close to this limit. This provides direct evidence that the persistent emission associated with FRB 121102 originates from a strong compact radio source.

## 3. PERSISTENT EMISSION AND ROTATION MEASURE OF FAST RADIO BURSTS

In Table 1, we list ten FRBs from the FRB catalog of Petroff et al. (2016) with the measured RM and the measured values (or upper limits) of the persistent emission

<sup>1</sup> The RM contributed by relativistic electrons would be suppressed by a factor of  $\gamma^2$ , where  $\gamma$  is the Lorentz factor of the electrons (Quataert & Gruzinov 2000).

TABLE 1  
FRB SAMPLE WITH MEASUREMENTS (OR UPPER LIMITS) OF RM AND PERSISTENT EMISSION FLUX

FRB Name	DM <sub>obs</sub> (pc cm <sup>-3</sup> )	DM <sub>MW</sub> <sup>a</sup> (pc cm <sup>-3</sup> )	z <sup>b</sup>	d <sub>L</sub> (Gpc)	RM (rad m <sup>-2</sup> )	F <sub>ν, RM</sub> <sup>c</sup> (μJy)	F <sub>ν</sub> <sup>d</sup> (μJy)	ν (GHz)	L <sub>ν</sub> (10 <sup>29</sup> erg s <sup>-1</sup> Hz <sup>-1</sup> )	References
FRB 121102	557	188	0.19273	0.98	1.4 × 10 <sup>5</sup>	698	180	1.7	2.1	1,2,3,4
FRB 180916	348.76	200	0.0337	0.15	-114.6	24.4	< 18	1.6	< 0.0048	5,6
FRB 180924	361.42	40.5	0.3214	1.74	14	0.022	< 20	6.5	< 0.72	7
FRB 181112	589.27	102	0.47550	2.76	10.9	0.0068	< 21	6.5	< 1.91	8
FRB 110523	623.3	43.52	0.58 <sup>+0.21</sup> <sub>-0.21</sub>	3.5 <sup>+1.6</sup> <sub>-1.4</sub>	-186.1	0.073 <sup>+0.129</sup> <sub>-0.038</sub>	< 40	0.8	< 5.8 <sup>+6.6</sup> <sub>-3.7</sub>	9
FRB 150215	1105.6	427.2	0.69 <sup>+0.22</sup> <sub>-0.22</sub>	4.3 <sup>+1.7</sup> <sub>-1.6</sub>	1.5	0.00039 <sup>+0.00060</sup> <sub>-0.00019</sub>	< 6.48	10.1	< 1.4 <sup>+1.4</sup> <sub>-0.9</sub>	10
FRB 150418	776.2	188.5	0.59 <sup>+0.21</sup> <sub>-0.21</sub>	3.6 <sup>+1.6</sup> <sub>-1.4</sub>	36	0.013 <sup>+0.022</sup> <sub>-0.007</sub>	< 70	1.4	< 11 <sup>+12</sup> <sub>-7</sub>	11
FRB 150807	266.5	36.9	0.17 <sup>+0.10</sup> <sub>-0.11</sub>	0.85 <sup>+0.57</sup> <sub>-0.57</sub>	12	0.08 <sup>+0.65</sup> <sub>-0.05</sub>	< 240	5.5	< 2.1 <sup>+3.7</sup> <sub>-1.8</sub>	12
FRB 160102	2596.1	13	3.04 <sup>+0.51</sup> <sub>-0.48</sub>	26.4 <sup>+5.4</sup> <sub>-4.9</sub>	-220.6	0.0015 <sup>+0.0008</sup> <sub>-0.0005</sub>	< 30	5.9	< 249 <sup>+112</sup> <sub>-84</sub>	13,14
FRB 180309	263.42	44.69	0.16 <sup>+0.10</sup> <sub>-0.10</sub>	0.79 <sup>+0.57</sup> <sub>-0.51</sub>	< 150	< 1.2 <sup>+8.0</sup> <sub>-0.8</sub>	< 105	2.1	< 0.8 <sup>+1.5</sup> <sub>-0.7</sub>	15

<sup>a</sup>From FRB catalog (Petroff et al. 2016).

<sup>b</sup>For FRB 121102, FRB 180916, FRB 180924 and FRB 181112, their redshifts are from the redshift measurements of their host galaxies (Chatterjee et al. 2017; Tendulkar et al. 2017; Bannister et al. 2019; Marcote et al. 2020; Prochaska et al. 2019). For other FRBs, their redshifts are inferred by the extragalactic DMs, i.e., Eq.(5). The redshift errors are given by  $\sigma_{\text{IGM}}$  from the IGM fluctuation (McQuinn 2014). For FRB 160102, due to its redshift is out of the range given by McQuinn (2014), we assume that  $\sigma_{\text{IGM}} = 350 \text{ pc cm}^{-3}$ .

<sup>c</sup>The predicted flux density given by RM, i.e., Eq.(3).

<sup>d</sup>For the FRBs without persistent emission detected, the upper limits correspond to the  $3\sigma$  flux density limits.

References: (1) Spitler et al. (2014); (2) Tendulkar et al. (2017); (3) Marcote et al. (2017); (4) Michilli et al. (2018); (5) CHIME/FRB Collaboration et al. (2019b); (6) Marcote et al. (2020); (7) Bannister et al. (2019); (8) Prochaska et al. (2019); (9) Masui et al. (2015); (10) Petroff et al. (2017); (11) Keane et al. (2016); (12) Ravi et al. (2016); (13) Bhandari et al. (2018); (14) Caleb et al. (2018); (15) Osłowski et al. (2019).

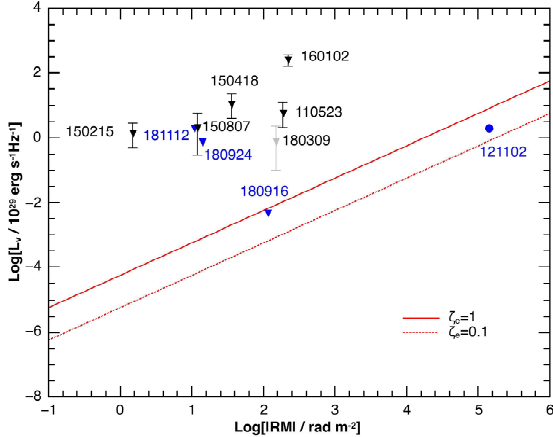


FIG. 1.— The relation between specific luminosity of persistent emission and RM of FRBs. The red solid line and dotted line denote the predicted relation for  $\zeta_e = 1$  and  $\zeta_e = 0.1$ , respectively. The black down-triangle points correspond to the FRBs with an upper limit of the persistent emission and a measured value of RM. The gray down-triangle point corresponds to the FRB with upper limits of RM and persistent emission. The circle point (FRB 121102) corresponds to the FRB with measured values of the persistent emission flux and RM. The blue points corresponds to the FRBs with precise localizations.

flux. Among them, only FRB 121102 has the measured values of both. The parameters in Table 1 include observed DM, DM contributed by Milky Way, estimated redshift based on DM and the corresponding luminosity distance, RM, predicted flux of the persistent emission based on Eq.(3), observed flux of the persistent emission, the frequency of the persistent emission, and the specific luminosity of the persistent emission.

For some FRBs, the persistent emission flux was constrained in a wide frequency range. We take the minimum value of the upper limits of the persistent emission flux density, because the predicted maximum flux density given by Eq.(3) is independent of fre-

quency. FRB 121102, FRB 180916, FRB 180924 and FRB 181112 have precise localizations (Chatterjee et al. 2017; Tendulkar et al. 2017; Bannister et al. 2019; Marcote et al. 2020; Prochaska et al. 2019), so the redshifts in Table 1 are the directly measured values. For other FRBs, due to the lack of precise localization, we estimate their redshifts and luminosity distances via the extragalactic DM, i.e.,  $\text{DM}_E = \text{DM}_{\text{obs}} - \text{DM}_{\text{MW}} = \text{DM}_{\text{IGM}} + \text{DM}_{\text{HG}}$ , where  $\text{DM}_{\text{obs}}$  is the observed total DM, and  $\text{DM}_{\text{MW}}$ ,  $\text{DM}_{\text{IGM}}$ , and  $\text{DM}_{\text{HG}}$  are the DMs contributed by Milky Way, intergalactic medium (IGM), and the FRB host galaxy, respectively. In this work, the DMs contributed by Milky Way are taken from<sup>2</sup> the FRB catalog (Petroff et al. 2016), and we assume that the local DM contributed by FRB host galaxies is  $\text{DM}_{\text{HG,loc}} = 100 \text{ pc cm}^{-3}$  (e.g., Xu & Han 2015; Yang et al. 2017; Luo et al. 2018; Li et al. 2019b). The extragalactic DM is given by (Deng & Zhang 2014)

$$\text{DM}_E(z) = \frac{3cH_0\Omega_b f_{\text{IGM}}}{8\pi Gm_p} \int_0^z \frac{\chi(z)(1+z)dz}{[\Omega_m(1+z)^3 + \Omega_\Lambda]^{1/2}} + \frac{\text{DM}_{\text{HG,loc}}}{1+z}, \quad (5)$$

where the fraction of baryons in the IGM is  $f_{\text{IGM}} \sim 0.83$  (Fukugita et al. 1998; Shull et al. 2012), and the free electron number per baryon in the universe is  $\chi(z) \simeq 7/8$ . The  $\Lambda$ CDM cosmological parameters are taken as  $\Omega_m = 0.315 \pm 0.007$ ,  $\Omega_b h^2 = 0.02237 \pm 0.00015$ , and  $H_0 = 67.36 \pm 0.54 \text{ km s}^{-1} \text{ Mpc}^{-1}$  (Planck Collaboration et al. 2018).

In Figure 1, we plot the relation between the specific luminosity of the persistent emission and RM. The FRB data are taken from Table 1. We assume that the typical scale of the emission region is  $R \sim 0.01 \text{ pc}$  (corresponding to the timescale of flux variation of the persistent

<sup>2</sup> <http://frbcat.org/>

emission associated with FRB 121102) for other FRBs. According to Eq.(2), the red solid line corresponds to the predicted relation for  $\zeta_e = 1$ , and the red dotted line corresponds to the predicted relation for  $\zeta_e = 0.1$ . For FRB 121102 with  $|\text{RM}| \sim 10^5 \text{ rad m}^{-2}$ , the observed flux is closed to the predicted value for  $\zeta_e \sim (0.1 - 1)$ . For FRB 180916, the VLA observations shows that there is no co-incident persistent emission above a  $3\sigma$  rms noise level of  $18 \mu\text{Jy}$  per beam at 1.6 GHz (Marcote et al. 2020). Such an upper limit is close to the predicted flux density given by Eq.(3) for  $\zeta_e \sim 1$ . For other FRBs, the upper limits of the observed flux densities are significantly higher than the predicted persistent emission flux density.

#### 4. DISCUSSION AND CONCLUSION

So far, both persistent radio emission and a large RM value are discovered only in FRB 121102. Although the persistent emission is found to be spatially coincident with the repeating bursts, it does not show a direct physical connection with the FRB 121102 bursting source (Chatterjee et al. 2017; Marcote et al. 2017; Tendulkar et al. 2017). In this work, we find a linear positive relation between the specific luminosity and RM (Eq.2). Such a relation is indeed satisfied for FRB 121102, given that the following conditions are satisfied:

- the persistent emission of FRB 121102 and its large RM originate from the same region;
- the magnetic field that contributes to RM and the persistent emission is coherent in large-scale (i.e.  $\zeta_B \sim 1$ );
- the ratio between relativistic and non-relativistic electrons in the emission region,  $\zeta_e$ , is of the order of unity.

If these conditions are satisfied for all other FRBs, we would expect that most FRBs with  $|\text{RM}| \lesssim \text{a few} \times 100 \text{ rad m}^{-2}$  (e.g., Petroff et al. 2017; Bhandari et al. 2018; Caleb et al. 2018; Osłowski et al. 2019; Bannister et al. 2019) would not have a detectable persistent emission counterpart. This seems to be consistent with the current observations. A deviation of the

prediction Eq.(2) would suggest that at least one of the above conditions is not satisfied. For example, a bright persistent emission source with relatively small RM would suggest that the magnetic field in the persistent emission region is mostly random.

The large-scale magnetic field requirement offers insight into the FRB mechanism. A large-scale magnetic field has been discovered near supermassive black holes or active galactic nuclei (Eatough et al. 2013; Michilli et al. 2018). It was also hypothesized to exist in shocked nebula (e.g., SNR, PWN, etc.) surrounding a magnetized neutron star (e.g., Metzger et al. 2019; Margalit & Metzger 2018). For the latter scenario, the synchrotron maser FRB mechanism requires that the magnetic fields lie in the plane of the shock. Such a field configuration needs to be destroyed to produce a radially ordered  $B$  field in the region where RM is generated.

As shown in Appendix, for more general setups, e.g.  $n_e \propto r^{-\alpha}$  and  $B \propto r^{-\beta}$ , for a given  $|\text{RM}|$ , the predicted flux of persistent emission is of the same order or slightly lower than that given by Eq.(3) for the uniform case. The observations of the persistent emission and RM of FRB 121102 imply that  $\alpha + \beta < 1$ , which is close to the uniform distribution assumption. FRB 180916 (Marcote et al. 2020), on the other hand, has an persistent emission flux upper limit very close to the predicted  $\text{DM}-L_{\nu, \text{max}}$  relation, suggesting that either  $\zeta_e < 1$ , or a smaller emission region ( $R < 0.01 \text{ pc}$ ), or a stratified medium with  $\alpha + \beta > 1$ .

Finally, different from DM measurements that require transients, RM measurements could be made for persistent sources as long as they are polarized. According to our analysis, the persistent emission region for FRB 121102 carries an ordered  $B$  field, so that its emission should be linearly polarized. We suggest a direct measurement of RM of the persistent emission of FRB 121102 to test our prediction.

We thank Qiancheng Liu, and Xiaohui Sun for helpful discussions.

#### APPENDIX

##### RELATION BETWEEN PERSISTENT EMISSION AND ROTATION MEASURE

In this appendix, we perform a more general treatment on the relation between the persistent emission specific flux and the RM of FRBs. We assume that at the radius  $r_0 < r < R$  from the FRB source, the electron number density follows  $n_e = n_{e,0}(r/r_0)^{-\alpha}$  and the magnetic field follows  $B = B_0(r/r_0)^{-\beta}$ . Then the RM is given by

$$|\text{RM}| = \frac{e^3 \xi_B}{2\pi m_e^2 c^4} \int_{r_0}^R B(r) n_e(r) dr = \begin{cases} \frac{e^3 \xi_B}{2\pi m_e^2 c^4} B_0 n_{e,0} R \left(\frac{R}{r_0}\right)^{-(\alpha+\beta)}, & \text{for } \alpha + \beta < 1, \\ \frac{e^3 \xi_B}{2\pi m_e^2 c^4} B_0 n_{e,0} r_0, & \text{for } \alpha + \beta > 1. \end{cases} \quad (\text{A1})$$

In the radius range  $r \sim r + dr$ , the radiation power of a single electron is  $P_\nu(r) = m_e c^2 \sigma_T B(r)/3e$ , and the number of electrons is  $4\pi r^2 \zeta_e n_e(r) dr$ . The observed peak flux at the distance  $D$  from the source is

$$F_{\nu, \text{max}} = \frac{1}{4\pi D^2} \int_{r_0}^R P_\nu(r) 4\pi r^2 \zeta_e n_e(r) dr = \frac{m_e c^2 \sigma_T \zeta_e B_0 n_{e,0}}{3e D^2} \times \begin{cases} \frac{R^3}{3 - (\alpha + \beta)} \left(\frac{R}{r_0}\right)^{-(\alpha+\beta)}, & \text{for } \alpha + \beta < 3, \\ \frac{r_0^3}{3 - (\alpha + \beta)}, & \text{for } \alpha + \beta > 3. \end{cases} \quad (\text{A2})$$



According to Eq.(A1) and Eq.(A3), one finally has

$$F_{\nu, \max} = \frac{16\pi^2}{9(3 - \alpha - \beta)} m_e c^2 \frac{\zeta_e}{\xi_B} \frac{R^2}{D^2} |\text{RM}| \times \begin{cases} 1, & \text{for } \alpha + \beta < 1, \\ \left(\frac{R}{r_0}\right)^{1-(\alpha+\beta)}, & \text{for } 1 < \alpha + \beta < 3, \\ \left(\frac{R}{r_0}\right)^{-2}, & \text{for } \alpha + \beta > 3. \end{cases} \quad (\text{A3})$$

This result is consistent with the uniform case with  $\alpha = \beta = 0$ . For any value of  $\alpha + \beta$ , one always has

$$F_{\nu, \max} \leq \frac{16\pi^2}{9(3 - \alpha - \beta)} m_e c^2 \frac{\zeta_e}{\xi_B} \frac{R^2}{D^2} |\text{RM}|. \quad (\text{A4})$$

The equal sign corresponds to the case with  $\alpha + \beta < 1$ .

#### REFERENCES

- Bannister, K. W., Deller, A. T., Phillips, C., et al. 2019, *Science*, 365, 565
- Bhandari, S., Keane, E. F., Barr, E. D., et al. 2018, *MNRAS*, 475, 1427
- Caleb, M., Keane, E. F., van Straten, W., et al. 2018, *MNRAS*, 478, 2046
- Chatterjee, S., Law, C. J., Wharton, R. S., et al. 2017, *Nature*, 541, 58
- CHIME/FRB Collaboration, Amiri, M., Bandura, K., et al. 2019a, *Nature*, 566, 235
- CHIME/FRB Collaboration, Andersen, B. C., Bandura, K., et al. 2019b, *ApJ*, 885, L24
- CHIME/FRB Collaboration, Amiri, M., Bandura, K., et al. 2019c, *Nature*, 566, 230
- Dai, Z. G., Wang, J. S., & Yu, Y. W. 2017, *ApJ*, 838, L7
- Deng, W., & Zhang, B. 2014, *ApJ*, 783, L35
- Eatough, R. P., Falcke, H., Karuppusamy, R., et al. 2013, *Nature*, 501, 391
- Fonseca, E., Andersen, B. C., Bhardwaj, M., et al. 2020, *arXiv e-prints*, arXiv:2001.03595
- Fukugita, M., Hogan, C. J., & Peebles, P. J. E. 1998, *ApJ*, 503, 518
- Keane, E. F., Johnston, S., Bhandari, S., et al. 2016, *Nature*, 530, 453
- Kellermann, K. I., & Pauliny-Toth, I. I. K. 1969, *ApJ*, 155, L71
- Li, D., Zhang, X., Qian, L., et al. 2019a, *The Astronomer's Telegram*, 13064, 1
- Li, Q.-C., Yang, Y.-P., & Dai, Z.-G. 2020, *submit*
- Li, Y., Zhang, B., Nagamine, K., & Shi, J. 2019b, *ApJ*, 884, L26
- Lorimer, D. R., Bailes, M., McLaughlin, M. A., Narkevic, D. J., & Crawford, F. 2007, *Science*, 318, 777
- Luo, R., Lee, K., Lorimer, D. R., & Zhang, B. 2018, *MNRAS*, 481, 2320
- Marcote, B., Paragi, Z., Hessels, J. W. T., et al. 2017, *ApJ*, 834, L8
- Marcote, B., Nimmo, K., Hessels, J. W. T., et al. 2020, *Nature*, 577, 190
- Margalit, B., & Metzger, B. D. 2018, *ApJ*, 868, L4
- Masui, K., Lin, H.-H., Sievers, J., et al. 2015, *Nature*, 528, 523
- McQuinn, M. 2014, *ApJ*, 780, L33
- Metzger, B. D., Berger, E., & Margalit, B. 2017, *ApJ*, 841, 14
- Metzger, B. D., Margalit, B., & Sironi, L. 2019, *MNRAS*, 485, 4091
- Michilli, D., Seymour, A., Hessels, J. W. T., et al. 2018, *Nature*, 553, 182
- Murase, K., Kashiyama, K., & Mészáros, P. 2016, *MNRAS*, 461, 1498
- Ośłowski, S., Shannon, R. M., Ravi, V., et al. 2019, *MNRAS*, 488, 868
- Petroff, E., Barr, E. D., Jameson, A., et al. 2016, *PASA*, 33, e045
- Petroff, E., Burke-Spolaor, S., Keane, E. F., et al. 2017, *MNRAS*, 469, 4465
- Planck Collaboration, Aghanim, N., Akrami, Y., et al. 2018, *arXiv e-prints*, arXiv:1807.06209
- Prochaska, J. X., Macquart, J.-P., McQuinn, M., et al. 2019, *Science*, 365, aay0073
- Quataert, E., & Gruzinov, A. 2000, *ApJ*, 545, 842
- Ravi, V., Shannon, R. M., Bailes, M., et al. 2016, *Science*, 354, 1249
- Ravi, V., Catha, M., D'Addario, L., et al. 2019, *Nature*, 572, 352
- Shull, J. M., Smith, B. D., & Danforth, C. W. 2012, *ApJ*, 759, 23
- Spitler, L. G., Cordes, J. M., Hessels, J. W. T., et al. 2014, *ApJ*, 790, 101
- Tendulkar, S. P., Bassa, C. G., Cordes, J. M., et al. 2017, *ApJ*, 834, L7
- Thornton, D., Stappers, B., Bailes, M., et al. 2013, *Science*, 341, 53
- Wang, J.-S., & Lai, D. 2019, *arXiv e-prints*, arXiv:1907.12473
- Xu, J., & Han, J. L. 2015, *Research in Astronomy and Astrophysics*, 15, 1629
- Yang, Y.-H., & Dai, Z.-G. 2019, *ApJ*, 885, 149
- Yang, Y.-P., Luo, R., Li, Z., & Zhang, B. 2017, *ApJ*, 839, L25
- Yang, Y.-P., Zhang, B., & Dai, Z.-G. 2016, *ApJ*, 819, L12
- Zhang, B. 2018, *ApJ*, 854, L21
- Zhang, Y. G., Gajjar, V., Foster, G., et al. 2018, *ApJ*, 866, 149